2018 International Conference on Unmanned Aircraft Systems (ICUAS)
Dallas, TX, USA, June 12-15, 2018

Comparison of Euler Estimate using Extended Kalman Filter, Madgwick and Mahony on Quadcopter Flight Data

Simone A. Ludwig[1] and Kaleb D. Burnham[2]

***Abstract*— A magnetic and inertial measurement unit (MIMU) provides raw, real-time acceleration, angular velocity, and a measure of earth's magnetic field. By itself, this data is subject to significant noise, bias, and drift (without constant re-calibration). A data fusion algorithm can be applied to significantly reduce these errors. In the past, many approaches have been adopted for filtering gyroscope data with inertial measurements, and the most commonly used techniques are Extended Kalman filtering and complementary filters. Thus, this paper compares three methods: two complementary filters known as Madgwick and Mahony, and the Extended Kalman Filter (EKF). Simulation experiments are conducted using quadcopter data and results show that Mahony provides better orientation estimation than both Madgwick and EKF when using optimum parameters.**

I. Introduction

With the recent rise of quadcopters and related micro-aerial vehicles, much research has been conducted to improve the localization accuracy of these objects. Improved accuracy is a precursor to creating autonomous agents for a variety of purposes and may lead to larger autonomous units such as commercial aircraft. Localization systems typically have two main components: onboard inertial measurement units (IMU) and the external global positioning system (GPS). IMUs provide short term position and orientation changes, though without expensive calibration, which are subject to rapid drift due to noise, bias, non-orthogonality, etc. However, fusion algorithms exist to reduce the effects of noise and bias on the data. GPS provides accurate long-term data but is subject to signal blocking and the multipath problem. For these reasons it is desirable to reduce the dependency on GPS. Microelectromechanical (MEMS) IMUs have become popular due to their low power consumption, light weight, and low cost.

In our previous work we have compared Madgwick, Mahony, and a basic DLR-AHRS filter [1]. The dataset was a simulant of a person's foot while walking. Since it was simulated data, gaussian distributed error was added to the gyroscope and accelerometer readings. No error was added to the magnetometer since it was assumed there were no magnetic disturbances and that its readings were reliable. Experiments were conducted with and without the error. In both cases, the Madgwick filter significantly outperformed the Mahony and DLR-AHRS approach. However, there is concern that since the dataset was so periodic the orientation may have been easier to predict than an object flying freely through space.

In [2], the Madgwick filter was tested against a Kalman Filter implementation. Three-axis MIMUs collected raw data. A Vicon system and Nexus software provided ground truth values. The experiment involved rotating the sensor 90 degrees around an axis, 180 degrees in the opposite direction, and 90 degrees to bring it back to the origin. This was repeated multiple times around each axis and the sensor was held stationary for 3 to 5 seconds between each rotation. This experiment achieved better results than a Kalman filter. However, the data set is too simplistic; it was meant only to validate the filter's method and is not representative of an object in motion. Without positional offset, the gravity vector is much easier to estimate accurately. Most applications of IMUs do not have such slow and smooth motion.

Cirillo et al. [3] has investigated the accuracy of an Extended Kalman Filter (EKF), Madgwick, and Mahony using a KUKA Youbot on an omnidirectional platform. Data was collected in two phases. The first phase consisted of rotating the three axes individually. In the second, joints were coordinated to rotate around multiple axes simultaneously. All three algorithms were implemented in Simulink. The authors conclude that the filters perform similarly, though the EKF has a higher computational load. They note that the extra computation is due to its generality, allowing additional sensory information to be added without redesigning or retuning parameters.

This paper uses flight data of a quadcopter and compares the Extended Kalman Filter (EFK) with Madgwick and Mahony to estimate an object's orientation. Each approach is evaluated and compared using RMSE (Root Mean Square Error) and the absolute error of the Euler estimates. Furthermore, the running time of all approaches are evaluated.

II. Background to Magnetic and Inertial Measurement Unit (MIMU)

This section describes magnetic and inertial measurement units and the method used to estimate attitude. Sources of error are briefly discussed, and the mathematical notation used in the rest of the paper is defined.

A. MIMU Sensor

MIMUs are a version of an inertial measurement unit (IMU) with a 3-axis magnetometer included. These are

[1]North Dakota State University, Fargo, ND, USA simone.ludwig@ndsu.edu
[2]North Dakota State University, Fargo, ND, USA

sometimes also referred to as an IMU, but for clarification the acronym has been extended. Data was collected using MEMS (microelectromechanical system) sensors. MEMS sensors are inexpensive and consequently suffer from many sources of error, including high levels of noise, bias, axis misalignment, scale factor, and local temperature [4].

Due to these errors, any of the sensors alone are not enough to accurately estimate attitude. Thus, their data is combined to produce a superior estimate of the MIMUs attitude. By combining readings from all three sensors, the cumulative effects of their errors can be significantly reduced.

1) Gyroscope: Gyroscopes directly measure rate of rotation, typically in $\frac{rad}{s}$. Integrating these values give an attitude estimation, however, without repetitive calibration this estimation can become so poor as to become unusable. For this paper, the velocity is represented as: $[s_{w_x} \quad s_{w_y} \quad s_{w_z}]^T$.

The continuous time model for a gyroscope can be expressed as:

$$s_w = s_{w_r} + s_{w_b} + s_{w_n} \tag{1}$$

where s_w is the angular rate measured by the gyroscope, s_{w_r} is the true angular rate, s_{w_b} is the gyroscope bias that models its derivative by a random walk noise, and s_{w_n} is the white noise of the gyroscope.

2) Accelerometer: Accelerometers measure the sum of gravity and acceleration of the MIMU in $\frac{m}{s^2}$. Only the gravity vector is useful for attitude estimation, and thus another estimate must be made to separate the gravity and acceleration vectors. This step is done within the filter. The gravity estimate is used to improve pitch and roll angle estimates. Acceleration is represented as $s_a = [s_{a_x} \quad s_{a_y} \quad s_{a_z}]^T$. The continuous time model of the accelerometer can be summarized as:

$$s_a = s_{a_r} + s_{a_b} + s_{a_n} \tag{2}$$

where s_a is the sum of the gravity and external acceleration of the tracking object, s_{a_r} is the sum of the gravity and external acceleration, s_{a_b} is the accelerometer bias that models its derivative by a Gauss-Markov noise, s_{a_n} is the accelerometer white noise.

3) Magnetometer: Magnetometers measure the magnetic field around the MIMU in μT. Of the three sensors, magnetometers suffer the least amount from inherent noise. With accurate readings, the yaw angle can be easily estimated. However, magnetometers are greatly influenced by local magnetic fields. Please refer to [5] for more information. Its readings are represented as $s_m = [s_{m_x} \quad s_{m_y} \quad s_{m_z}]^T$. The continuous time model of the magnetometer is represented as:

$$s_m = s_{m_r} + s_{m_b} + s_{m_n} \tag{3}$$

where s_m is the magnetic field measured by the magnetometer, s_{m_r} is the true magnetic field, s_{m_b} is the bias of the magnetometer where its derivative is modeled by a Gauss-Markov noise, and s_{m_n} is the white noise.

B. Attitude Representation

Calculations of a MIMU's orientation are typically done with unit quaternions. These link the local frame of the MIMU with with Earth's frame. Accuracy depends entirely on how well these frames are aligned. Other representations include Euler angles and 3x3 direction cosine matrices (DCM) [6]. Euler angles are useful when viewing data but are ambiguous and suffer from the gimbal lock during calculations [7]. DCMs are stable but are slower to calculate as nine values need to be computed each update compared to four for quaternions. Thus, quaternions are the popular choice. They are defined as [8]:

$$q = S_{E_q} = \begin{bmatrix} q_0 \\ \overrightarrow{q} \end{bmatrix} = [q_0 \quad q_1 \quad q_2 \quad q_3]^T \in \Re^4 \tag{4}$$

where q_0 and $\overrightarrow{q}$ are the scalar and the vector portions of the quaternion, respectively.

Since quaternions are less intuitive to interpret, this paper converts final values into Euler angles. These are comprised of three rotations [7]:

- a rotation φ around the x-axis (roll angle)
- a rotation θ around the y-axis (pitch angle)
- a rotation ψ around the z-axis (yaw angle)

III. Attitude Estimation Algorithms

The overall design of attitude estimation filters including the Mahony filter [9], Madgwick Filter [10], and EKF [11] descriptions are provided in the following subsections.

A. Filter Design

The Mahony and Madgwick algorithms are described using common notations used for quaternion and their sensor readings. The estimated vector v is described by $\hat{v} = [\hat{v}_x \quad \hat{v}_y \quad \hat{v}_z]^T$, the quaternion and angular rate errors are given by q_e, w_e, and the time difference between two epochs is $\triangle t$.

In order to estimate q, the two filter algorithms use two reference vectors E_a and E_m for acceleration and magnetic field, respectively. For the static case, $E_a = [0 \quad 0 \quad g]^T$ where g is the acceleration due to gravity ($g \approx 9.8\frac{m}{s^2}$). If there are no magnetic deviations, then E_m can be calculated as described in [12]. In a noise-free environment, the relation can be described as:

$$s_{a_q} = q^{-1} \otimes E_{a_q} \otimes q \tag{5}$$

where $\otimes$ is the quaternion multiplication [8]. s_{a_q} is the quaternion form of s_a, which can be described by $S_{a_q} = [0 \quad s_{a_x} \quad s_{a_y} \quad s_{a_z}]^T$. E_{a_q} is the quaternion form of E_a.

In a perfect, noise-free, no-magnetic-deviation environment, the relation between E_m and s_m is as follows:

$$s_{m_q} = q^{-1} \otimes E_{m_q} \otimes q \tag{6}$$

where s_{m_q} is the quaternion form of s_m, which can be given as $s_{m_q} = [0 \quad s_{m_x} \quad s_{m_y} \quad S_{m_z}]^T$. E_{m_q} is the quaternion form of E_m.

The kinematic equation of a rigid body is given by angular velocity measurements from a gyroscope in order to describe the variations of the attitude in terms of quaternions such as:

$$\dot{q} = \frac{1}{2} q \otimes s_{w_q} \tag{7}$$

where s_{w_q} is the quaternion of s_w.

B. Mahony Filter

Algorithm 1 displays the equations used for the Mahony filter. Please note that k_i and k_p are the integral and proportional adjustable gains (see Equation 1), respectively. The algorithm computes the error by cross multiplying the measured and the estimated vectors, and the acceleration and magnetic field. This then allows to correct the gyroscope bias.

Algorithm 1 Mahony Filter [9]

$s_{\hat{a}_{q,t}} = \hat{q}_{t-1}^{-1} \otimes E_{a_{q,t}} \otimes \hat{q}_{t-1}$
$s_{\hat{m}_{q,t}} = \hat{q}_{t-1}^{-1} \otimes E_{m_{q,t}} \otimes \hat{q}_{t-1}$

$s_{w_{mes,t}} = [s_{a_t} \times s_{\hat{a}_t}] + [s_{m_t} \times s_{\hat{m}_t}]$
$s_{\dot{\hat{w}}_{b,t}} = -k_i s_{w_{mes,t}}$
$s_{\hat{w}_{r,q,t}} = s_{w_{q,t}} - [0 \quad s_{\hat{w}_{b,t}}] + [0 \quad k_p s_{w_{mes,t}}]$

$\dot{\hat{q}} = \frac{1}{2} \hat{q}_{t-1} \otimes s_{\hat{w}_{r,q,t}}$

C. Madgwick Filter

The Madgwick filter algorithmic description is given in Algorithm 2. Madgwick is a gradient descent based algorithm. In this algorithm, the quaternion error calculation from the gradient descent algorithm provides also a gyroscope drift compensation. J_t describes the Jacobian Matrix of F_t, β is the divergence rate of q_t representing the magnitude of a quaternion derivative according to the gyroscope measurement error, and ζ is the integral gain.

Algorithm 2 Madgwick Filter [10]

$E_{\hat{h}_{q,t}} = \hat{q}_{t-1} \otimes s_{m_{q,t}} \otimes \hat{q}_{t-1}^{-1}$
$E_{\hat{m}_{q,t}} = [0 \quad 0 \quad \sqrt{E_{\hat{h}_{x,t}^2} + E_{\hat{h}_{y,t}^2}} \quad E_{\hat{h}_{z,t}}]^T$
$F_t = \begin{bmatrix} \hat{q}_{t-1}^{-1} \otimes E_{a_{q,t}} \otimes \hat{q}_{t-1} - s_{a_{q,t}} \\ \hat{q}_{t-1}^{-1} \otimes E_{m_{q,t}} \otimes \hat{q}_{t-1} - s_{m_{q,t}} \end{bmatrix}$
$\hat{q}_{e,t} = J_t^T F_t$

$s_{\hat{w}_{e,t}} = 2\hat{q}_{t-1} \otimes \hat{q}_{e,t}$
$s_{\dot{\hat{w}}_{b,t}} = s_{w_{e,t}}$
$s_{\hat{w}_t} = s_{w_t} - \zeta s_{w_{b,t}}$

$\dot{\hat{q}}_t = \frac{1}{2} \hat{q}_{t-1} \otimes s_{\hat{w}_{q,t}} - \beta \frac{\hat{q}_{e,t}}{||\hat{q}_{e,t}||}$

D. Extended Kalman Filter (EKF)

The Extended Kalman filter is a closed loop system consisting of the following four steps:

1) Prediction
2) Kalman gain
3) Update
4) Quaternion normalization

The MIMU sensor input is provided during the update step, and after each of the four steps are executed, the output is provided in the form of an estimated orientation.

The Extended Kalman filter is used to model nonlinear systems, which deal with cases that are governed by nonlinear stochastic differential equations such as:

$$\dot{\mathbf{x}} = \mathbf{f}(\mathbf{x}, t) + \mathbf{u}(t) \tag{8}$$

$$\mathbf{z} = \mathbf{h}(\mathbf{x}, t) + \mathbf{v}(t) \tag{9}$$

where $\mathbf{u}(t)$ and $\mathbf{v}(t)$ are white noise sequences with zero means, which are mutually independent:

$$\begin{aligned} E[\mathbf{u}(t)\mathbf{u}^T(\tau)] = q\delta(t-\tau); \quad E[\mathbf{v}(t)\mathbf{v}^T(\tau)] \\ = r\delta(t-\tau); \quad E[\mathbf{u}(t)\mathbf{v}^T(\tau)] = \mathbf{0} \end{aligned} \tag{10}$$

where $\delta(t)$ is the Dirac delta function, $E[\cdot]$ is the expectation, and superscript T represents the matrix transpose.

In the discrete-time equivalent form, Equations (8) and (9) are given as:

$$\mathbf{x}_{k+1} = \mathbf{f}(\mathbf{x}_k, k) + \mathbf{w}_k \tag{11}$$

$$\mathbf{z}_k = \mathbf{h}(\mathbf{x}_k, k) + \mathbf{v}_k \tag{12}$$

where $\mathbf{x}_k \in \Re^n$ is the state vector, $\mathbf{w}_k \in \Re^m$ is the process noise vector, $\mathbf{z}_k \in \Re^m$ measurement vector, and $\mathbf{v}_k \in \Re^m$ measurement noise vector. In Equations (11) and (12), $\mathbf{w}_k$ and $\mathbf{v}_k$ are zero mean Gaussian white noise sequences that are having zero cross-correlation with each other such as:

$$\mathbf{E}[\mathbf{w}_k \mathbf{w}_i^T] = \mathbf{Q}_k \delta_{ik} \tag{13}$$

$$\mathbf{E}[\mathbf{v}_k \mathbf{v}_i^T] = \mathbf{R}_k \delta_{ik} \tag{14}$$

$$\mathbf{E}[\mathbf{w}_k \mathbf{v}_i^T] = 0 \quad for \quad all \quad i \quad and \quad k \tag{15}$$

where $\mathbf{Q}_k$ is the process noise covariance matrix, and $\mathbf{R}_k$ is the measurement noise covariance matrix. The Kronecker delta function δ_{ik} is described by:

$$\delta_{ik} = \begin{cases} 1, & i = k \\ 0, & i \neq k \end{cases} \tag{16}$$

The Extended Kalman Filter algorithmic description is given in Algorithm 3. Equations (17) - (19) are measurement update equations, whereas Equations (20) - (22) are time update equations from step k to $k+1$. In order to calculate

an improved posteriori estimation, the equations transform the measurement value into a priori estimation. $\mathbf{P}_k$ is the error covariance matrix defined by $\mathbf{E}[(\mathbf{x}_k - \hat{\mathbf{x}}_k)(\mathbf{x}_k - \hat{\mathbf{x}}_k)^T]$, for which $\hat{\mathbf{x}}_k$ is an estimate of the system state vector $\mathbf{x}_k$ and $\mathbf{K}_k$ is the Kalman gain matrix. The algorithm starts with initial condition values $\hat{\mathbf{x}}_0^-$ and $\mathbf{P}_0^-$ and once a new measurement $\mathbf{z}_k$ becomes available, the estimation of states and the corresponding error covariance are calculated recursively. More details on the Extended Kalman Filter are given in [13], [14], [15].

Algorithm 3 Extended Kalman Filter Algorithm

1. Initialization of the state vector and state covariance matrix:

$$\hat{\mathbf{x}}_\mathbf{0}^- \quad and \quad \mathbf{P}_\mathbf{0}^-$$

2. Computation of the Kalman gain matrix:

$$\mathbf{K}_k = \mathbf{P}_k^- \mathbf{H}_k^T [\mathbf{H}_k \mathbf{P}_k^- \mathbf{H}_k^T + \mathbf{R}_k]^{-1} \tag{17}$$

3. The state correction vector and update state vector are calculated as follows:

$$\hat{\mathbf{x}}_k = \hat{\mathbf{x}}_\mathbf{k}^- + \mathbf{K}_k[\mathbf{z}_k - \hat{\mathbf{z}}_k^-], \quad with \quad \hat{\mathbf{z}}_k^- = \mathbf{h}(\hat{\mathbf{x}}_k^-, k) \tag{18}$$

4. Update of error covariance:

$$\mathbf{P}_k = [\mathbf{I} - \mathbf{K}_k \mathbf{H}_k] \mathbf{P}_k^- \tag{19}$$

5. Prediction of new state vector and state covariance matrix:

$$\hat{\mathbf{x}}_{k+1}^- = \mathbf{f}(\hat{\mathbf{x}}_k, k) \tag{20}$$

$$\mathbf{P}_{k+1}^- = \mathbf{\Phi}_k \mathbf{P}_k \mathbf{\Phi}_k^T + \mathbf{Q}_k \tag{21}$$

where the linear approximation equations for the system and measurement matrices are obtained as follows:

$$\mathbf{\Phi}_k \approx \frac{\partial \mathbf{f}_k}{\partial \mathbf{x}}\Big|_{\mathbf{x}=\hat{\mathbf{x}}_k^-}; \quad \mathbf{H}_k \approx \frac{\partial \mathbf{h}_k}{\partial \mathbf{x}}\Big|_{\mathbf{x}=\hat{\mathbf{x}}_k^-} \tag{22}$$

IV. Experiments and Results

This section describes the parameter setup of the estimation algorithm first followed by the description of the data set used and the evaluation measures applied. The fourth subsection lists the experimental simulation results in figures and tables.

A. Parameter Setup for Algorithms

Optimum parameter values for Madgwick and Mahony were obtained using a genetic algorithm since these are extremely sensitive and even minor changes can give drastically different results. More details on the use of a genetic algorithm for parameter optimization can be found in [16]. Thus, the following values have been identified:

- Madgwick: $\beta = 0.011765$
- Mahony: $k_p = 0.0039216$ and $k_i = 0.001$

The initial parameters in the Extended Kalman Filter were not optimally estimated since they quickly converge to the best value. All algorithms are implemented in MATLAB.

B. Data Set

The data set was obtained from [17]. The sensor data represents the motion of a quadcopter as it travels in a rectangular path. To remain consistent with previous work, angular velocities are bounded from 180 to 180 degrees. To deal with issues of signs changing along the boundaries, absolute values are taken for all error calculations. Ground truth Euler angles were collected using a Vicon system. In particular, the datasets were recorded using an AscTec 'Pelican' quadrotor (see Figure 1), flying in an indoor environment of size $10m \times 10m \times 10m$.

Figure 2 shows the trajectory traveled by the quadrotor, tracked by the motion capture system, during the '1loop' experiment (2D top view (left) and 3D side view (right) of the trajectory traveled by the quadrotor during the '1LoopDown' experiment). The data sets include acceleration and angular velocity readings from the IMU.

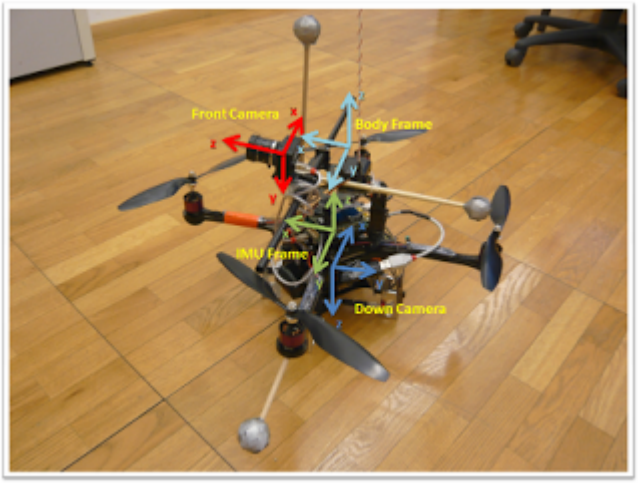

Fig. 1. Quadrotor frames [18]

C. Evaluation Measures

Euler angles are typically used to represent orientation with roll, pitch, and yaw. However, they can be subject to ambiguity and gimbal lock. To remove those issues, Madgwick and Mahony use quaternions to represent orientation in three-dimensions. These are converted back into Euler angles for error calculations. The Root Mean Square Error (RMSE) and the mean absolute error are used as a measure of accuracy. We evaluate the accuracy of Madgwick, Mahony, and the Extended Kalman Filter. Furthermore, the execution time of each is evaluated.

D. Results of Simulation Experiments

Figures 3-5 and Table I shows the results of the Euler estimation for all three filters. As can be seen by the table and the figures, the three filters achieve similar results. It

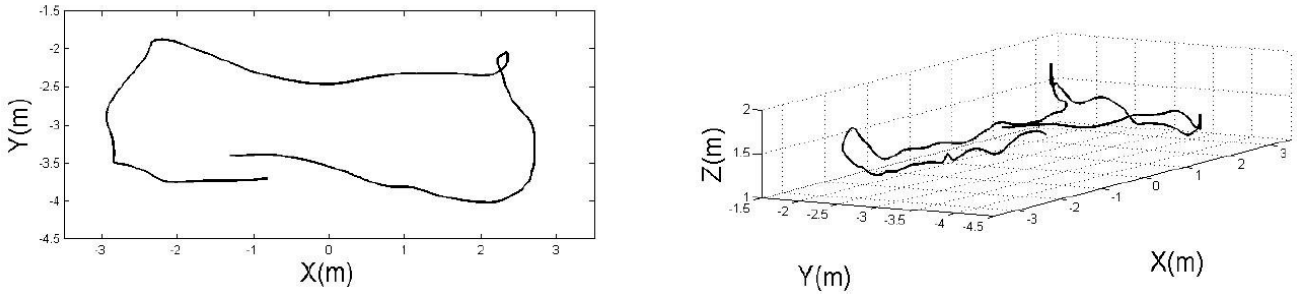

Fig. 2. Quadrotor during "1loop" experiment [19]

is important to note that the large jumps from 180 degrees to 180 degrees did not affect the error calculations. Of the three algorithms, Mahony achieved the smallest RMSE with a norm of 11.0107 degrees. The Extended Kalman Filter performed the worst in this regard. However, it is useful to note that the mean absolute error at each sample gives a different ordering.

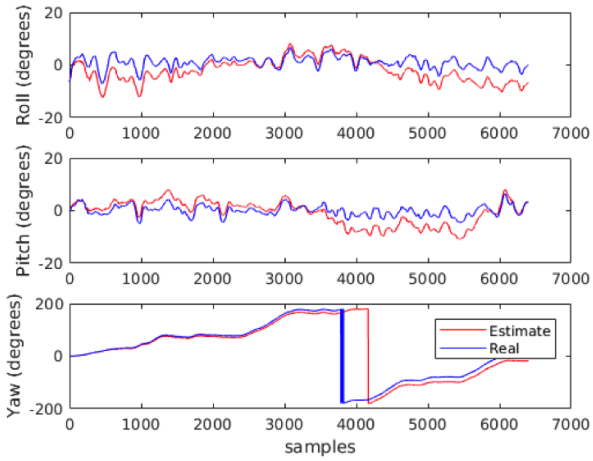

Fig. 3. Euler Estimates of Madgwick

TABLE I
RMSE OF EULER ESTIMATES

	X	Y	Z	Norm
Madgwick	3.4677	3.3482	12.0775	13.0039
Mahony	4.1204	4.7005	9.06644	11.0107
EKF	1.4088	1.2055	13.1648	13.2948

TABLE II
MEAN ABSOLUTE ERROR OF EULER ESTIMATES

	X	Y	Z	Sum
Madgwick	1.2272	1.8787	3.6674	6.7733
Mahony	1.0723	1.0605	4.2376	6.3704
EKF	0.2220	0.2397	5.3192	5.7809

While all three filters appear to give comparable results using both error measures (Table I and II), Madgwick and

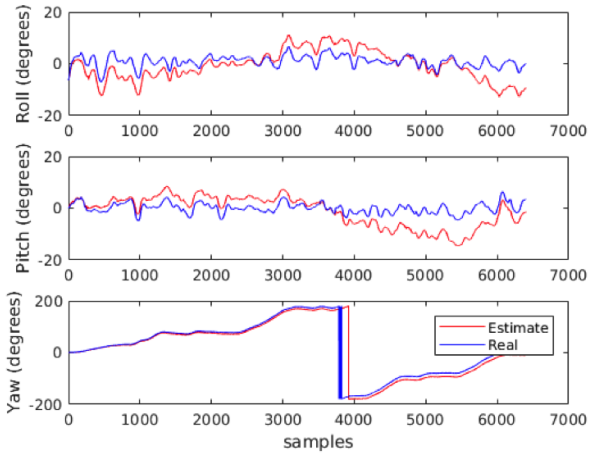

Fig. 4. Euler Estimates of Mahony

Mahony require sensitive parameters that appear to be unique to each data set or type of motion. Initial parameters in the Kalman filter are less important since they quickly change to dynamically reduce gain.

In all three filters, the yaw estimate was significantly more inaccurate than the other axes. Since this is largely determined by the magnetometer data, we conclude that there were magnetic disturbances in the data collection room causing the sensor to detect more information than solely the earth's magnetic field. In an ideal setup, the norm measurement of earth's magnetic field should remain constant. However, there were significant fluctuations in this value indicating magnetic disturbances.

Finally, the execution time needed to update each filter through all the samples is compared. There are $6,401$ samples in our data set.

TABLE III
RUNTIME IN SECONDS FOR 3 ESTIMATION ALGORITHMS

	Execution time (seconds)
Madgwick	0.2080
Mahony	0.1782
EKF	0.2895

As can be seen in Table III, Mahony achieved the fastest execution time (0.1782 seconds) with the EKF performing

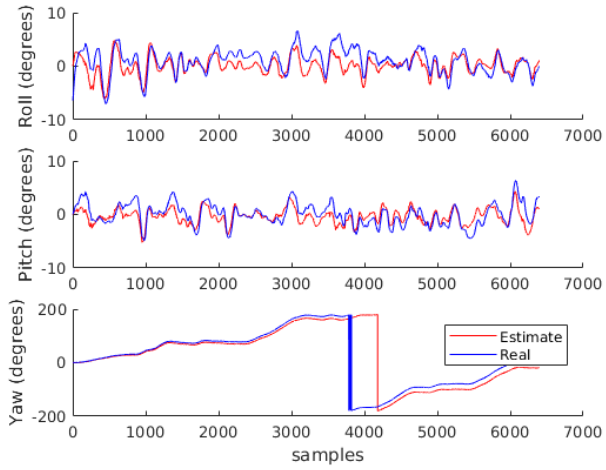

Fig. 5. Euler Estimates of EKF

the slowest (0.2895 seconds). This is expected since the EKF is more general and easily able to accommodate more information, such as barometric pressure sensors or GPS.

V. Conclusion

The recent rise of quadcopters and related micro-aerial vehicles has led to more research being conducted to improve the localization accuracy of these objects. Improved accuracy is a necessity for creating autonomous agents for different purposes, and this may lead to larger autonomous units such as commercial aircrafts.

A magnetic and inertial measurement unit (MIMU) provides raw, real-time acceleration, angular velocity, and a measure of earth's magnetic field. By itself, this data is subject to significant noise, bias, and drift. However, fusing acceleration, angular velocity, and magnetometer readings provides a far more accurate orientation estimation. This paper compares the accuracy of the Madgwick, Mahony, and Extended Kalman Filter in estimating orientation of a moving object. Data was collected by a quadcopter with ground truth obtained using a Vicon system. Euler angle estimations were compared to the ground truth and the error was measured using Root-Mean-Square Error and the mean absolute error. In addition, the execution time of each was evaluated.

The three filters achieved relatively similar results using both error measurements with Mahony outperforming Madgwick and EKF. In terms of execution time, Mahony had the fastest execution time with the EKF performing the slowest. This is expected, however, due to a higher computational load.

Acknowledgment

This work is funded by North Dakota Department of Commerce under project number FAR0027254.

References

[1] S. A. Ludwig, K. D. Burnham, A. R. Jimnez, P. A. Touma, Comparison of attitude and heading reference systems using foot mounted MIMU sensor data: basic, Madgwick, and Mahony, SPIE Conference on Sensors and Smart Structures Technologies for Civil, Mechanical, and Aerospace Systems, Denver, CO, USA, March 2018.

[2] R. Mahony, Tarek Hamel, Jean-Michel Pflimlin. Nonlinear Complementary Filters on the Special Orthogonal Group. IEEE Transactions on Automatic Control, Institute of Electrical and Electronics Engineers, 53 (5), pp. 1203-1217, 2008.

[3] A. Cirillo, P. Cirillo, G. De Maria, C. Natale, and S. Pirozzi. A comparison of multisensor attitude estimation algorithms. Multisensor Attitude Estimation: Fundamental Concepts and Applications, Chapter: 29, Publisher: CRC Press, Editors: H. Fourati, D. E. C. Belkhiat, pp. 529-539, 2016.

[4] T. Michel, H. Fourati, P. Geneves, N. Layada. A Comparative Analysis of Attitude Estimation for Pedestrian Navigation with Smartphones. 2015 International Conference on Indoor Positioning and Indoor Navigation, Banff, Canada, October 2015.

[5] W. M. Chung, S. Yeung, W. W. Chan, R. Lee, Validity of VICON Motion Analysis System for Upper Limb Kinematic Measurement A Comparison Study with Inertial Tracking Xsens System. Hong Kong Physiother. J. 2011.

[6] D. Sachs, Sensor fusion on android devices: A revolution in motion processing, [Video] https://www.youtube.com/watch?v=C7JQ7Rpwn2k, 2010, [Online; last accessed December 2017].

[7] J. Diebel, Representing attitude: Euler angles, unit quaternions, and rotation vectors, Matrix, vol. 58, pp. 15-16, 2006.

[8] B. Kuipers, Quaternions and rotation sequences, vol. 66, 1999.

[9] R. Mahony, T. Hamel, and J.-M. Pflimlin, Nonlinear complementary filters on the special orthogonal group, Automatic Control, IEEE Transactions on, vol. 53, no. 5, pp. 1203-1218, 2008.

[10] S. O. Madgwick, A. J. Harrison, and R. Vaidyanathan, Estimation of IMU and MARG orientation using a gradient descent algorithm, in 2011 IEEE International Conference on Rehabilitation Robotics (ICORR), 2011.

[11] J. L. Marins, X. Yun, E. R. Bachmann, R. B. McGhee, and M. J. Zyda. Extended kalman filter for quaternion-based orientation estimation using marg sensors. In Proc. of the 2001 IEEE/RSJ Int. Conf. on Intelligent Robots and Systems, pages 2003-2011, 2001.

[12] NGA and the U.K.'s Defence Geographic Centre (DGC), The world magnetic model, http://www.ngdc.noaa.gov/geomag/WMM, 2015, [Online; last accessed December 2017].

[13] R. Brown, P. Hwang, P. Introduction to Random Signals and Applied Kalman Filtering, Wiley, New York, NY, 1997.

[14] J. A. Farrell, M. Barth, The Global Positioning System & Inertial Navigation, McGraw-Hill, New York, NY, 1999.

[15] A. Gelb, Applied Optimal Estimation, MIT Press, Cambridge, MA, 1974.

[16] S. A. Ludwig, A. R. Jimnez, Optimization of Gyroscope and Accelerometer/Magnetometer Portion of Basic Attitude and Heading Reference System, Proceedings of 2018 IEEE International Symposium on Inertial Sensors and Systems (INERTIAL), Lake Como, Italy, March 2018.

[17] G. H. Lee, M. Achtelik, F. Fraundorfer, M. Pollefeys, and R. Siegwart, A Benchmarking Tool for MAV Visual Pose Estimation, International Conference on Control, Automation, Robotics and Vision (ICARCV'10), Singapore, December, 2010.

[18] MAV DataSet, https://sites.google.com/site/gimheelee/home/mavdataset, last retrieved February 2018.

[19] R. G. Valenti, I. Dryanovski, J. Xiao, Keeping a Good Attitude: A Quaternion-Based Orientation Filter for IMUs and MARGs, Sensors 2015, 15(8), 19302-19330, 2015.